ACS EARTH AND SPACE CHEMISTRY

ACS AUTHORCHOICE

http://pubs.acs.org/journal/aesccq

Letter

Commensurate Growth of Magnetite Microinclusions in Olivine under Mantle Conditions

Marcello Campione,* Mattia La Fortezza, Matteo Alvaro, Marco Scambelluri, and Nadia Malaspina*

Cite This: *ACS Earth Space Chem.* 2020, 4, 825−830

Read Online

ACCESS | Metrics & More | Article Recommendations | Supporting Information

ABSTRACT: Magnetite-bearing multiphase solid inclusions hosted in metamorphic olivine have been interpreted as final products of the trapping of the aqueous fluid produced by the subduction-zone dehydration of former serpentinites. We provide here a careful analysis performed by microfocus single-crystal X-ray diffraction of inclusions found in harzburgites from the Almirez Complex (Bétic Cordillera, Spain) to determine the occurrence of preferential crystallographic orientation relationships between the olivine host and the magnetite inclusion. The results demonstrate that the magnetite−olivine interface selectively displays parallelism between crystallographic planes (111) and (100) and between crystallographic directions ⟨110⟩ and ⟨011⟩, respectively. This evidence points to a clear epitaxial growth of magnetite on olivine. The calculation of the geometrical misfit between the two lattices in contact as a function of their relative azimuthal orientation shows that, under the aforementioned reciprocal orientation, a perfect commensurism is achieved; i.e., all of the nodes of the magnetite lattice coincide with nodes of the olivine lattice. This particular relationship must be interpreted as a unique occurrence, playing a fundamental role in favoring the heterogeneous nucleation of magnetite on olivine.

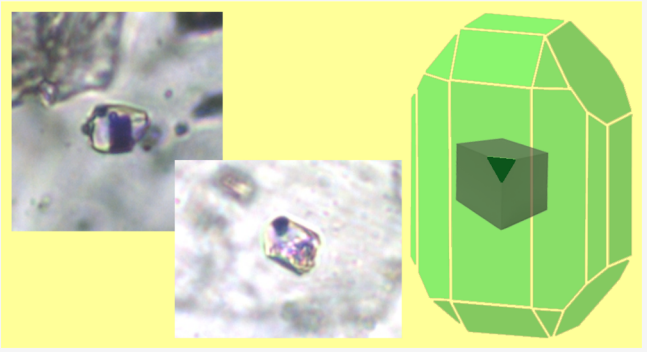

KEYWORDS: *serpentinization, dehydration reaction, nucleation and growth, epitaxy, X-ray diffraction, reciprocal crystallographic orientations*

INTRODUCTION

Fluid inclusions trapped in minerals equilibrated or recrystallized at high pressures in the deep Earth (pressure p > 1 GPa) are remnants of the fluid phases released during dehydration reactions of minerals or by fluid−rock interaction. This type of inclusion is commonly hosted by minerals that are themselves the product of the fluid-related geologic process, such as, for instance, olivine forming by serpentine dehydration in subducted serpentinites. During subduction, the water stored in serpentinites is progressively released at increasing temperatures by the following sequence of dehydration reactions: (1) Chrysotile ± lizardite + $SiO_{2(aq)}$ = antigorite + fluid occurs during early subduction (p < 1 GPa; temperature T = 200−300 °C) beneath accretionary wedges, up to 30 km depth. (2) Antigorite + brucite = olivine + fluid occurs at eclogite facies conditions (p = 1−2 GPa; T = 300−500 °C) during the prograde subduction metamorphism up to 60 km depth. Evidence of this reaction has been described in alpine serpentinites from Erro Tobbio (Liguria, Italy), which show rock- and vein-forming antigorite + olivine paragenesis and the occurrence of Cl-, B-, and Li-bearing fluid inclusions in olivine and diopside.[1,2] (3) Antigorite = olivine + orthopyroxene + chlorite + fluid occurs at p > 2 GPa and T > 550 °C, corresponding to subduction depths exceeding 60 km in the mantle. It represents the most important dehydration reaction, releasing 5−10 wt % of H_2O in the overlying mantle wedge.[3]

Here, we investigate natural multiphase inclusions produced by the antigorite breakdown reaction 3 hosted in chlorite harzburgites from Cerro del Almirez (Spain) and related to the subduction-zone dehydration of serpentinite protoliths that formed the fossil Jurassic oceanic lithosphere involved in the alpine orogeny.[4] In these rocks, olivine produced by reaction 3 hosts several multiphase inclusions characterized by enrichments in B, Li, alkalis, Pb, and Sr.[5]

The so-called multiphase inclusions generally correspond to regular microcavities in metamorphic minerals, which contain a mix of microcrystalline minerals (daughter phases) wet by a fluid phase; they are traditionally interpreted as either the result of direct precipitation of the solute dissolved in the fluid or the result of a more complex interaction between the fluid and the host mineral (dissolution−precipitation process). As a

Received: January 24, 2020
Revised: June 6, 2020
Accepted: June 8, 2020
Published: June 8, 2020

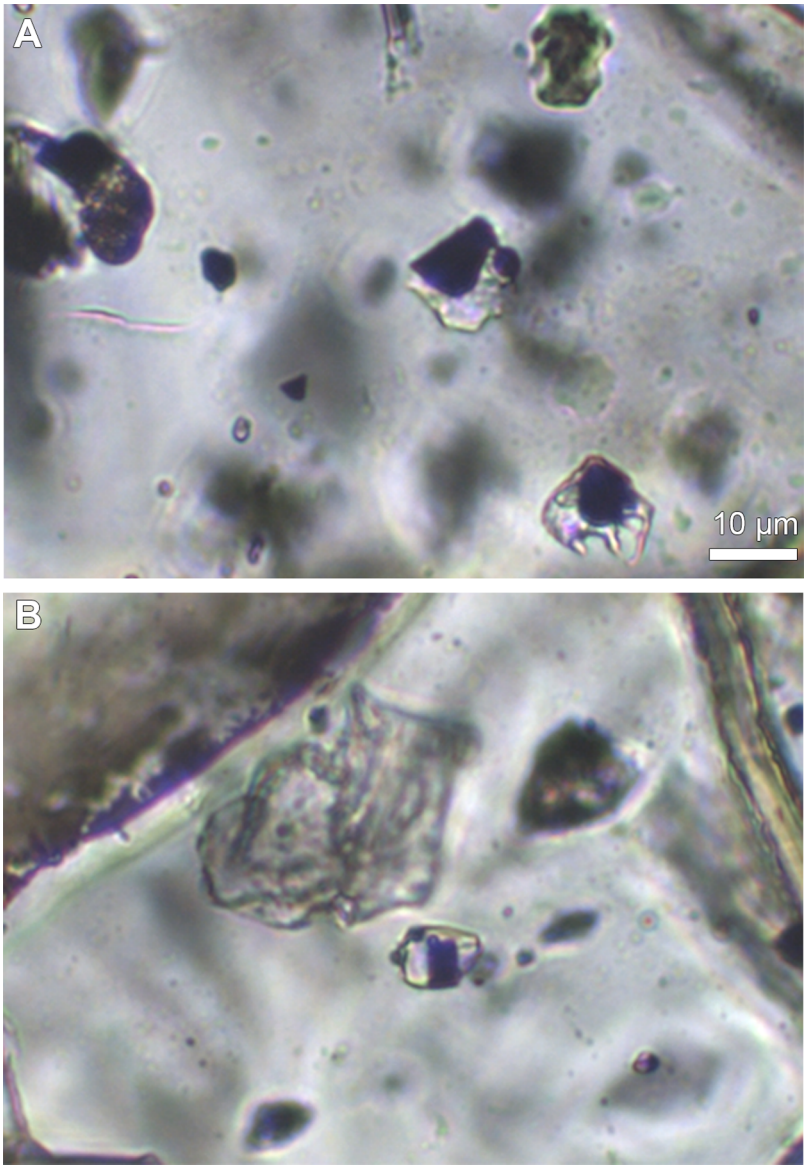

Figure 1. Optical micrographs of solid microinclusions in olivine. Magnetite microcrystals appear as an opaque phase with a cubic habit growing in contact with the olivine host mineral forming a cavity with a negative crystal shape. Constant volume ratios are observed between the various tiny solid inclusions and the residual fluid phase.

reference example, garnet−orthopyroxenite from the Maowu Ultramafic Complex (China) formed at ∼4 GPa and 750 °C as a result of metasomatism of former mantle harzburgite driven by a SiO_2- and H_2O-rich fluid phase. These rocks contain multiphase inclusions of the fluid evolved by the fluid−rock interaction process. Campione et al.[6] showed that the mineral assemblages inside the inclusions can be modeled in terms of thermodynamic equilibrium achieved among precipitated bulk solid phases immersed in liquid by taking into account special volume and mass constraints imposed by the host−inclusion system. Malaspina et al.[7,8] demonstrated for the first time the presence of an epitaxial registry between the precipitated spinel mineral infilling in a garnet host. Epitaxial registry requires that interface processes, such as heterogeneous nucleation, might have an important influence on the dynamics of phase nucleation and the mechanism that allows attaining thermodynamic equilibrium. To substantiate this hypothesis, here, we show that the inclusions in metamorphic olivine formed by serpentinite dehydration at Cerro del Almirez reveal a unique case of commensurate epitaxial growth at mantle conditions of the daughter phases in magnetite-bearing multiphase solid inclusions in olivine.

METHODOLOGY

Single-crystal diffractometry has been performed at the Department of Earth and Environmental Sciences of the University of Pavia using a Rigaku Oxford Diffraction SuperNova diffractometer equipped with a Mo microsource X-ray tube and a Dectris Pilatus-R200 K detector, controlled by the Crysalis-Pro software (Rigaku Oxford Diffraction). Centring of the inclusion and data collection have been performed by scanning φ (60°) with a scan width of 0.5°,[7,9] producing 120 frames with an exposure of 15 s. Measurements have been performed on pristine inclusions larger than 15 μm, for which the signal-to-noise ratio allowed for reliable measurements of the angular position of diffraction peaks and, thus, consistent determination of the orientation matrices

https://dx.doi.org/10.1021/acsearthspacechem.0c00026
ACS Earth Space Chem. 2020, 4, 825−830

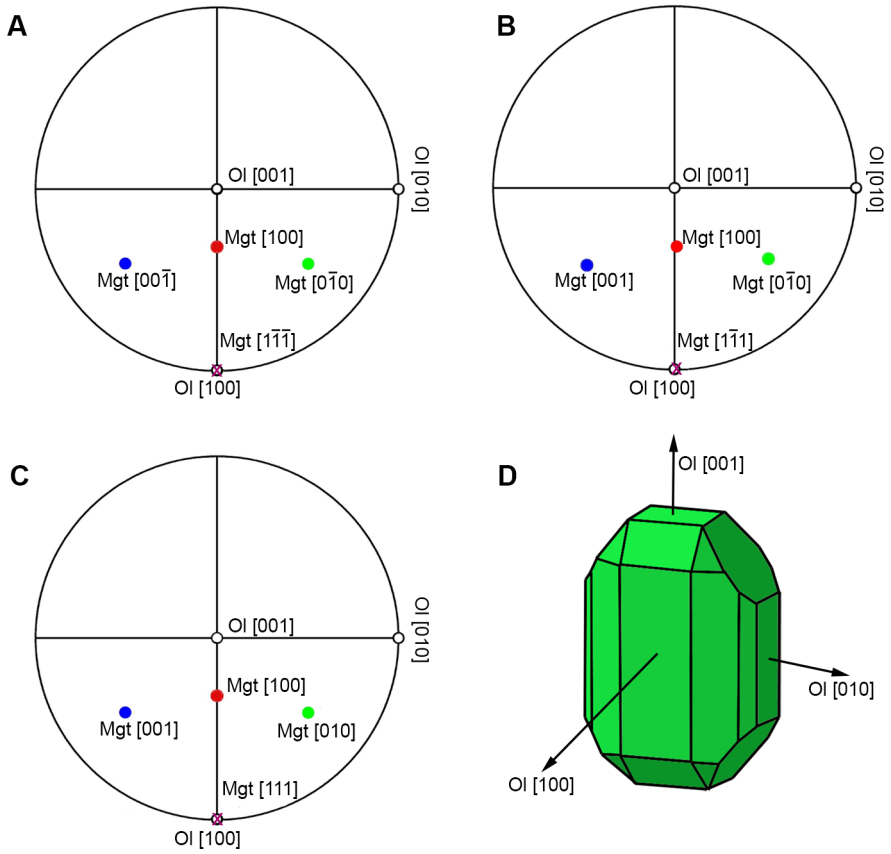

Figure 2. (A–C) Stereographic projections showing the orientation of magnetite inclusions relative to olivine host. (D) Olivine (Ol) host is plotted with (100), (010), and (001) planes (black open dots) oriented parallel to the *x*, *y*, and *z* axis, respectively. The magnetite (mgt) (111) plane (purple cross) is systematically observed to be parallel to Ol(100) with three symmetrically equivalent relative azimuthal orientations. This indicates that mgt(111) and Ol(100) are contact planes with a precise epitaxial registry. Blue, red, and green dots indicate mgt(001), mgt(100) and mgt(010) planes.

(see Table S1 of the Supporting Information). The orientation matrices have as components the reciprocal lattice vectors of the crystal with respect to the ϕ axis coordinate system of the diffractometer.[10] The orientation matrices of each host and inclusions come from one measurement; therefore, the orientation matrices for any host crystal and all of its guest crystals are of the same type. With the software OrientXplot,[11] one can process the two orientation matrices for each host inclusion pair and determine their relative crystallographic orientations (CORs). Furthermore, OrientXplot software has been used to remove the ambiguities in the indexing of the diffraction data by applying the known symmetry of both the inclusion and host crystals.[11,12] Stereographic projections then allow for the visualization and comparison of the reciprocal CORs among several inclusions contained in several hosts.

As already pointed out for Mg–chromite inclusions in diamond host, the full analyses of the CORs produced variations in the measured orientation of the major crystallographic axes of the inclusions relative to their hosts of less than 4° (see Table 2 in ref 12). This value provides an indication of the possible uncertainty on the measurements of inclusion–host relative orientations and a useful cutoff to discriminate significant misorientations.

EpiCalc software was used to model the geometric agreement between olivine and magnetite by calculating a dimensionless potential (V/V_0)[13] defined as follows. Surface lattices are modeled as overlapping plane waves with wavelength corresponding to surface lattice parameters. V/V_0 assumes discrete values between −0.5 and 1, according to the degree of matching between the substrate and overlayer for the given azimuthal angle θ, which is the angle included between the base vectors that define the meshes of the two lattices in contact. In our case, the substrate is represented by the olivine host, whereas the magnetite inclusion represents the overlayer. The values −0.5, 0, 0.5, and 1 are associated with a particular type of epitaxial register: for $V/V_0 = 1$, there will be incommensurate epitaxy; for $V/V_0 = 0.5$, there will be point-on-line (POL) coincidence; for $V/V_0 = 0$, there will be commensurate epitaxy [point-on-point (POP)]; and finally for $V/V_0 = -0.5$, there will be commensurate POL epitaxy in the case of a hexagonal substrate.[14] EpiCalc also generates the transformation matrix, which consists of a 2 × 2 square matrix that if multiplied to the vectors of the substrate lattice generates the vectors of the overlayer.

RESULTS AND DISCUSSION

The main microstructural feature of the studied Almirez samples is the presence of coarse, centimeter-sized, metamorphic olivine with an arborescent and "spinifex-like" texture grown in the presence of abundant aqueous fluid released by the antigorite dehydration reaction 3 (see Figure S1 of the Supporting Information). A first generation of olivine forms irregularly shaped clear cores, extensively overgrown by rims of a second generation of olivine with brown pleochroism as a result of the presence of numerous oriented nanoinclusions of

https://dx.doi.org/10.1021/acsearthspacechem.0c00026
ACS Earth Space Chem. 2020, 4, 825–830

magnetite, chromite, and ilmenite grown during the crystallization of olivine. The multiphase inclusions are found within both generations of olivine and show a regular negative crystal shape (Figure 1). They display several tiny solid, birefringent microcrystals, along with a fluid phase and a cubic-shaped, opaque phase constituted by magnetite, which is always observed to grow in contact with the cavity walls of the olivine host mineral. Previous works[15] identified the coexistence of chlorite and liquid water by Raman and scanning electron microscope analyses. Constant volume proportions are observed[15] among the various tiny solid inclusions inside the cavity (30% oxides as magnetite, 50% oxides as silicate, and 20% oxides as liquid).

Microfocused X-ray diffraction (XRD) was performed with the aim to characterize the crystal phases inside the inclusions by collecting diffraction patterns pertaining to a diffraction volume including all of the cavity volume and a fraction of the host nearby the cavity. The crystallographic data processing was performed by indexing the diffraction peaks to obtain the UB matrix (see ref 10 for further details). The UB matrices also enable the acquisition of the cell parameters of the phases (see Table S1 of the Supporting Information) that allow for identification of them as olivine and magnetite. By a combination of the information on the matrices of two phases, it was possible to establish their reciprocal CORs with the help of the program OrientXplot.[11] Figure 2 reports the outcome of this analysis with the help of stereographic projections.

We identified the occurrence of three symmetrically equivalent reciprocal orientations of magnetite and olivine. In these orientations, the magnetite(111) plane is always parallel to olivine(100). This indicates that the magnetite microcrystals grew with their (111) plane in contact with olivine(100). Given these contact planes, three different yet symmetrically equivalent azimuthal orientations of the two crystals are found. Indeed, primitive crystallographic directions of magnetite are observed to be parallel to three fixed directions.

To understand the selection of this orientation between magnetite and olivine, we assume this to be the result of an energetically favorable configuration arising from a possible lattice match between magnetite(111) and olivine(100). To analyze this match, we quantified the geometrical registry between the two lattices as a function of the azimuthal angle θ between the short surface axis of olivine and the surface axis of magnetite. This quantification was based on the algorithm used by the program EpiCalc. The results of this modeling performed for magnetite and olivine are displayed in Figure 3.

Clear minima of the dimensionless potential appear at $\theta = 0°$ and $\pm 60°$ (Figure 3A). Under these configurations, the triangular lattice of magnetite(111) is oriented in such a way that all of its lattice nodes are coincident with lattice nodes of olivine (Figure 3B). The transformation matrix converting olivine lattice base vectors into those of magnetite is characterized by all integer elements. This occurrence demonstrates achievement of perfect commensurate contacts between magnetite(111) and olivine(100). Considering the different symmetry and lattice metrics of the two crystals, this commensurate relationship appears as an exceptional occurrence. Lattice coincidences among mineral phases in inclusions were already found for the spinel/pyrope system.[7] However, such coincidences were of the POL type because only half of the lattice points of the overlaying spinel coincide with lattice points of the pyrope substrate. A POP coincidence (i.e., commensurism) as that observed in this study is the strongest and rarest form of lattice match.

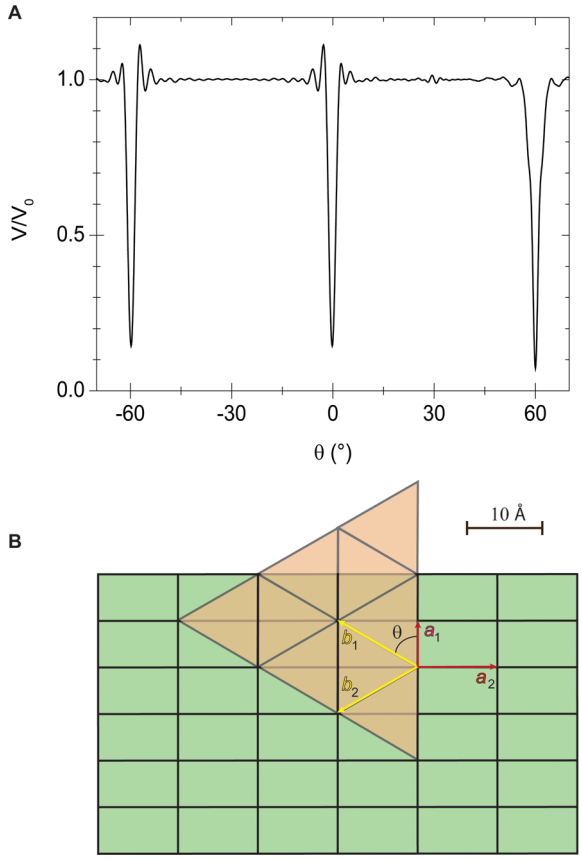

Figure 3. Geometric modeling of the agreement between magnetite and olivine deduced by calculating the lattice mismatch between magnetite(111) [brownish lattice with $b_1 = b_2 = 11.84$ Å] and olivine(100) [greenish lattice with $a_1 = 5.98$ Å and $a_2 = 10.23$ Å] as a function of the azimuthal orientation θ [angle between a_1 and b_1]. Calculation was performed with the program EpiCalc, which computes values of a dimensionless potential V/V_0 showing minima at angles θ ensuring a certain degree of coincidence among lattice points. (A) At $\theta = 0°$ and $\pm 60°$, the dimensionless potential is observed to decrease from 1.0 down to 0.0. This is the lowest possible value admitted and indicates commensurism of the two lattices. (B) Indeed, e.g., for $\theta = +60°$, the matrix allowing for the conversion of the olivine lattice base vectors into those of the magnetite lattice (transformation matrix) has all integer elements $\begin{pmatrix} \mathbf{b}_1 \\ \mathbf{b}_2 \end{pmatrix} = \begin{bmatrix} 1.00 & -1.00 \\ -1.00 & -1.00 \end{bmatrix} \begin{pmatrix} \mathbf{a}_1 \\ \mathbf{a}_2 \end{pmatrix}$, indicating that all lattice points of magnetite lie on lattice points of olivine.

Lattice match is commonly associated with an energetic advantage, in the sense that, when geometric coincidence is provided between two crystal surfaces in contact, this ensures maximization of attractive interactions and then minimization of the interface energy.

It is reasonable to suggest that the favorable interaction between olivine(100) and magnetite(111) reduces to a great extent the energy barrier for the heterogeneous nucleation of magnetite. This reduction is the primary cause for the kinetic selection of magnetite without which, under the same conditions, magnetite nucleation would probably have been suppressed. As a result of the exceptional occurrence of commensurism, this interaction might be so strong that magnetite nucleation can occur under a very low level of

https://dx.doi.org/10.1021/acsearthspacechem.0c00026
ACS Earth Space Chem. 2020, 4, 825−830

supersaturation or even at undersaturation of the fluids.[16] Commensurism is not the only way mineral infillings have been observed to organize at the host−cavity interface. For the case of garnet−orthopyroxenite from the Maowu Ultramafic Complex cited above,[7 and 8] a POL registry has been observed between spinel(100) and pyrope(100). There, the two crystals present the same cubic symmetry, with the square lattices in contact having different metrics. However, the lattice parameter of spinel(100) is a factor equal to $\sin(\pi/4)$ of that of pyrope, allowing for a coincident azimuthal orientation of the two lattices. Even though this coincidence plays a similar role in promoting the nucleation of spinel, it is not so robust as the commensurism observed in the magnetite−olivine system. These considerations demonstrate that, when studying multiphase inclusion systems with the purpose of deducing features of large-scale processes, it must be taken into account that interfaces might play a significant role in the formation process of mineral phases. This example of commensurate growth of magnetite on olivine demonstrates that interface energetics, together with volume properties of the minerals, control the physical appearance of reaction products. This represents a general conclusion and does not hold only within the unique environment of inclusion systems.

The studied inclusions are microsystems showing the chemical behavior of a subduction fluid during interaction with olivine in a closed system. Our study shows that the process of evolution of a fluid that is in contact with olivine is controlled by the reaction of magnetite formation as well as the energetic cost related to the nucleation and growth of the product phases. Our results show that, despite the crystallographic differences between magnetite and olivine, the availability of suitable lattice planes particularly facilitates the nucleation of product magnetites. This may explain the widespread occurrence of magnetite at sites of deserpentinization.

■ ASSOCIATED CONTENT

Supporting Information

The Supporting Information is available free of charge at https://pubs.acs.org/doi/10.1021/acsearthspacechem.0c00026.

Optical micrographs of peridotites (Figure S1) and XRD lattice parameters of olivine and magnetite (Table S1) (PDF)

■ AUTHOR INFORMATION

Corresponding Authors

Marcello Campione − *Department of Earth and Environmental Sciences, University of Milano—Bicocca, I-20126 Milano, Italy*; orcid.org/0000-0001-5627-6186; Email: marcello.campione@unimib.it

Nadia Malaspina − *Department of Earth and Environmental Sciences, University of Milano—Bicocca, I-20126 Milano, Italy*; orcid.org/0000-0002-7089-1035; Email: nadia.malaspina@unimib.it

Authors

Mattia La Fortezza − *Department of Earth and Environmental Sciences, University of Milano—Bicocca, I-20126 Milano, Italy*

Matteo Alvaro − *Department of Earth and Environmental Sciences, University of Pavia, I-27100 Pavia, Italy*

Marco Scambelluri − *Department of Earth Science, Environment, and Life, University of Genova, I-16132 Genova, Italy*

Complete contact information is available at: https://pubs.acs.org/10.1021/acsearthspacechem.0c00026

Notes

The authors declare no competing financial interest.

■ ACKNOWLEDGMENTS

Marcello Campione acknowledges the financial support of the University of Milano—Bicocca with FAQC Grant 2018-ATESP-0010. Nadia Malaspina, Matteo Alvaro, and Marco Scambelluri acknowledge the financial support of the Italian Ministry of University and Research (PRIN 2017, Prot. 2017ZE49E7_005). Matteo Alvaro is thankful to Marta Morana for her help in carrying our XRD experiments.

■ REFERENCES

(1) Scambelluri, M.; Piccardo, G. B.; Philippot, P.; Robbiano, A.; Negretti, L. High Salinity Fluid Inclusions Formed from Recycled Seawater in Deeply Subducted Alpine Serpentinite. *Earth Planet. Sci. Lett.* **1997**, *148* (3−4), 485−499.

(2) Scambelluri, M.; Tonarini, S. Boron Isotope Evidence for Shallow Fluid Transfer across Subduction Zones by Serpentinized Mantle. *Geology* **2012**, *40* (10), 907−910.

(3) Ulmer, P.; Trommsdorff, V. Serpentine Stability to Mantle Depths and Subduction-Related Magmatism. *Science* **1995**, *268* (5212), 858−861.

(4) Trommsdorff, V.; López Sánchez-Vizcaíno, V.; Gómez-Pugnaire, M. T.; Müntener, O. High Pressure Breakdown of Antigorite to Spinifex-Textured Olivine and Orthopyroxene, SE Spain. *Contrib. Mineral. Petrol.* **1998**, *132* (2), 139−148.

(5) Scambelluri, M.; Müntener, O.; Ottolini, L.; Pettke, T. T.; Vannucci, R. The Fate of B, Cl and Li in the Subducted Oceanic Mantle and in the Antigorite Breakdown Fluids. *Earth Planet. Sci. Lett.* **2004**, *222* (1), 217−234.

(6) Campione, M.; Tumiati, S.; Malaspina, N. Primary Spinel + Chlorite Inclusions in Mantle Garnet Formed at Ultrahigh-Pressure. *Geochemical Perspect. Lett.* **2017**, *4*, 19−23.

(7) Malaspina, N.; Alvaro, M.; Campione, M.; Wilhelm, H.; Nestola, F. Dynamics of Mineral Crystallization from Precipitated Slab-Derived Fluid Phase: First in Situ Synchrotron X-Ray Measurements. *Contrib. Mineral. Petrol.* **2015**, *169* (3), 1−12.

(8) Malaspina, N.; Langenhorst, F.; Tumiati, S.; Campione, M.; Frezzotti, M. L.; Poli, S. The Redox Budget of Crust-Derived Fluid Phases at the Slab-Mantle Interface. *Geochim. Cosmochim. Acta* **2017**, *209*, 70−84.

(9) Murri, M.; Cámara, F.; Adam, J.; Domeneghetti, M. C.; Alvaro, M. Intracrystalline "Geothermometry" Assessed on Clino and Orthopyroxene Bearing Synthetic Rocks. *Geochim. Cosmochim. Acta* **2018**, *227*, 133−142.

(10) Busing, W. R.; Levy, H. A. Angle Calculations for 3- and 4-Circle X-Ray and Neutron Diffractometers. *Acta Crystallogr.* **1967**, *22* (4), 457−464.

(11) Angel, R.; Milani, S.; Alvaro, M.; Nestola, F. OrientXplot: A Program to Analyse and Display Relative Crystal Orientations. *J. Appl. Crystallogr.* **2015**, *48* (4), 1330−1334.

(12) Nimis, P.; Angel, R. J.; Alvaro, M.; Nestola, F.; Harris, J. W.; Casati, N.; Marone, F. Crystallographic Orientations of Magnesiochromite Inclusions in Diamonds: What Do They Tell Us? *Contrib. Mineral. Petrol.* **2019**, *174* (4), 1−13.

(13) Last, J. A.; Hooks, D. E.; Hillier, A. C.; Ward, M. D. The Physicochemical Origins of Coincident Epitaxy in Molecular Overlayers: Lattice Modeling vs Potential Energy Calculations. *J. Phys. Chem. B* **1999**, *103* (32), 6723−6733.

(14) Hooks, D. E.; Fritz, T.; Ward, M. D. Epitaxy and Molecular Organization on Solid Substrates. *Adv. Mater.* **2001**, *13* (4), 227−241.
(15) Scambelluri, M.; Bottazzi, P.; Trommsdorff, V.; Vannucci, R.; Hermann, J.; Gòmez-Pugnaire, M. T.; Lòpez-Sànchez Vizcaìno, V. Incompatible Element-Rich Fluids Released by Antigorite Breakdown in Deeply Subducted Mantle. *Earth Planet. Sci. Lett.* **2001**, *192* (3), 457−470.
(16) Mutaftschiev, B. *The Atomistic Nature of Crystal Growth*; Hull, R., Osgood, R. M., Sakak, H., Zunger, A., Eds.; Springer: Berlin, Germany, 2001; Springer Series in Materials Science, Vol. *43*, DOI: 10.1007/978-3-662-04591-6.

https://dx.doi.org/10.1021/acsearthspacechem.0c00026
ACS Earth Space Chem. 2020, 4, 825−830